Supporting Information

NIR-II Light Triggered Nitric Oxide Release Nanoplatform Combined Chemo-Photothermal Therapy for Overcoming Multidrug Resistance Cancer

Jin Wang,[#] Canchen Wu,[#] Xiru Qin, Youyou Huang, Jianan Zhang, Tingting Chen, Yang Wang, Yue Ding,* Yong Yao**

School of chemistry and chemical engineering, Nantong University, Nantong, Jiangsu 226019, China.

E-mail: ywang85@ntu.edu.cn, yueding@ntu.edu.cn, yaoyong1986@ntu.edu.cn

[#]The authors contributed equally to the work.

1. Experimental Section

1.1 Materials.

Cetyltrimethyl ammonium bromide (CTAB), copper sulfate ($CuSO_4•5H_2O$, 99%), Selenium dioxide (SeO_2, 99.9%), vitamin C (Vc), Doxorubicin (DOX) hydrochloride, Tetraethylorthosilicate (TEOS) and N-[3-(Trimethoxysilyl)propyl]ethylenediamine (AEAPTS), folic acid (FA), N-(3-Dimethylaminopropyl)-N'-ethylcarbodiimide hydrochloride (EDC, 97%) and N-hydroxysuccinimide (NHS, 98%) were obtained from Aladdin Chemistry Co. Ltd. (Shanghai, China). DAF-FM DA was acquired from Beyotime Biotechnology. Anti-P-gp antibody (ab129450, Abcam), Dulbecco's modified eagle medium (DMEM, PAA Laboratories), fetal bovine serum (FBS, PAA Laboratories), hoechst33342 (Ultra Pure, Aldrich), and methylthiazolyldiphenyl-tetrazolium bromide (MTT, Ultra Pure, Aldrich) were used as received. MCF-7 (a human breast carcinoma cell line) and MCF-7/ADR (a human breast MDR cancer cell line) were received from Shanghai Institute of Biochemistry and Cell Biology.

1.2 Characterization.

Scanning electron microscopy (SEM) images were acquired on a ZEISS Gemini SEM 300. Transmission electron microscopy (TEM) observations were conducted on a FEI Talox F200X electron microscope at an acceleration voltage of 300 kV. The UV-Vis-NIR spectroscopy was recorded by using a Shimadzu UV3600 spectrophotometer. Super-resolution multiphoton confocal laserscanning microscopy (CLSM) was performed on a Leica TCS SP8 STED 3X instrument. The 808 nm and 1064 nm NIR irradiations were carried out by using a continuous wave diode laser (Changchun

Femtosecond Technology Co. Ltd., China). XRD was carried out by means of a Rigaku D/max-2550pc instrument with monochromatized CuKa radiation and a scanning step of 0.028.

2. Figures

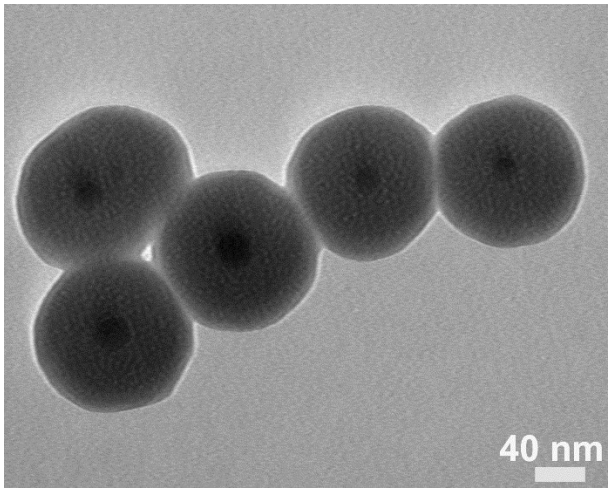

Fig. S1 TEM image of $Cu_{2-x}Se@SiO_2$ nanoparticles.

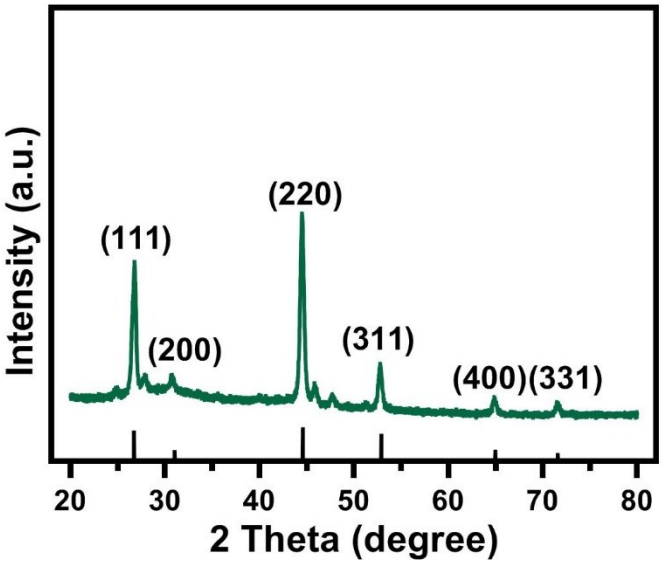

Fig. S2 X-ray diffraction patterns of CSNPs.

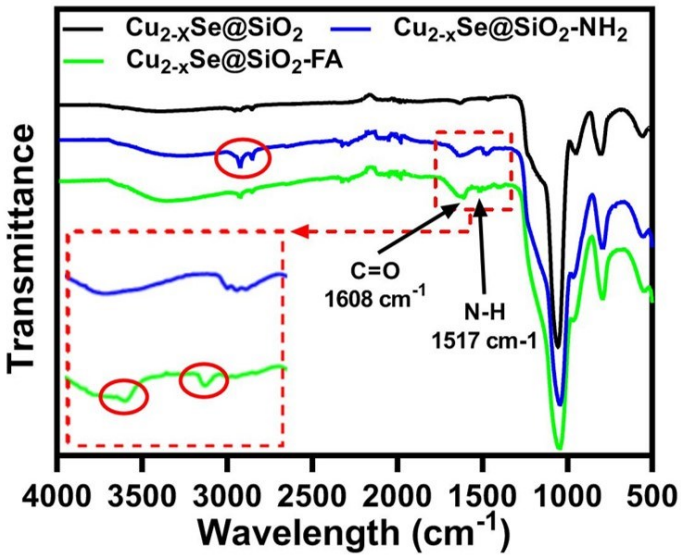

Fig. S3 Fourier-transform infrared (FT-IR) spectra of $Cu_{2-x}Se@SiO_2$, $Cu_{2-xSe}@SiO_2$-NH_2 and $Cu_{2-x}Se@SiO_2$-FA.

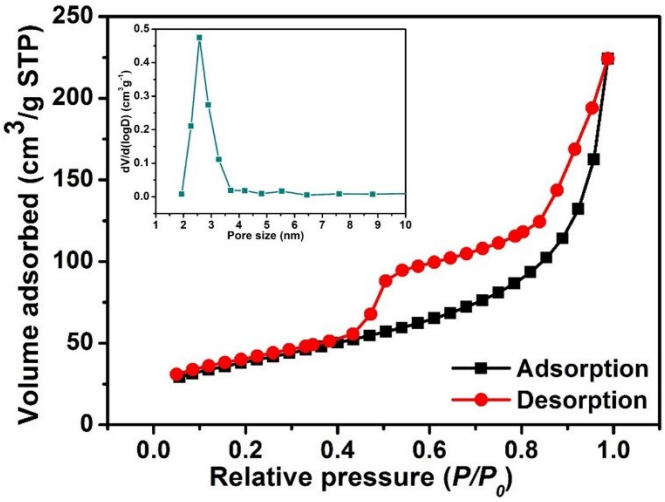

Fig. S4 Nitrogen adsorption-desorption isotherms and pore diameter distributions (inset).of CSNPs.

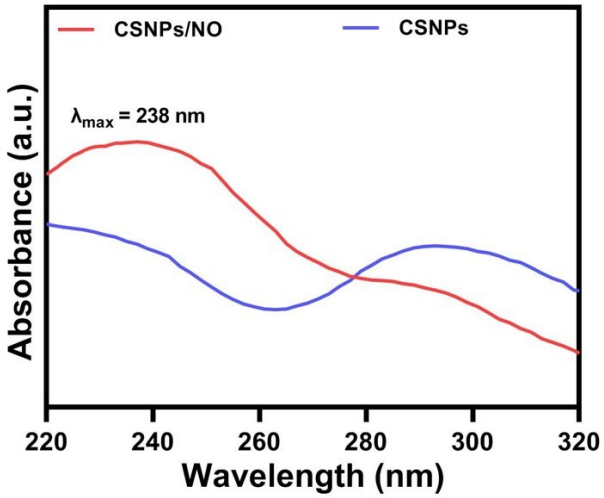

Fig. S5 UV-vis absorbance spectra of CSNPs and CSNPs/NO aqueous solution.

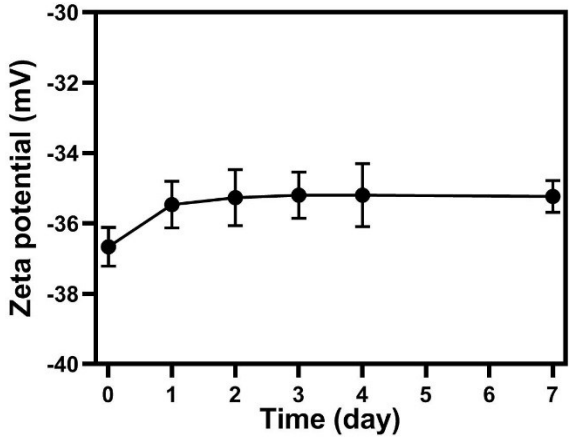

Fig. S6 Zeta potential of CSNPs/NO after storage in PBS solution (pH = 7.4) at room temperature. (n = 3 for each time point)

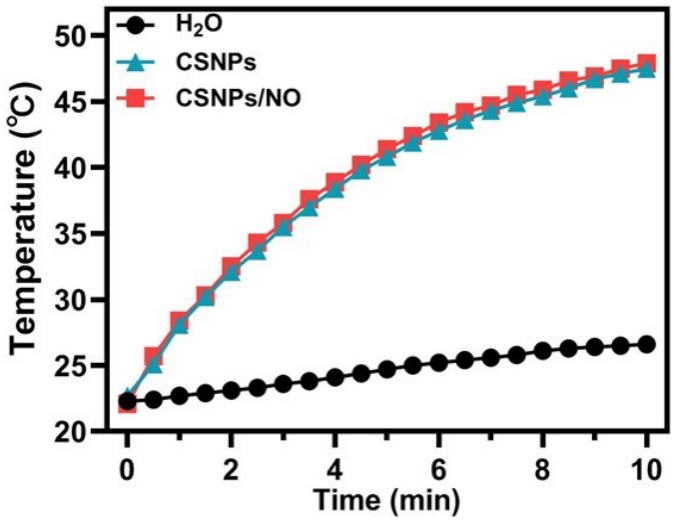

Fig. S7 Photothermal effects of the aqueous solution of CSNPs and CSNPs/NO at the same concentration (200 μg/mL) under 1064 nm laser irradiation (1.0 W/cm^2) for 10 min; pure water was used as a negative control.

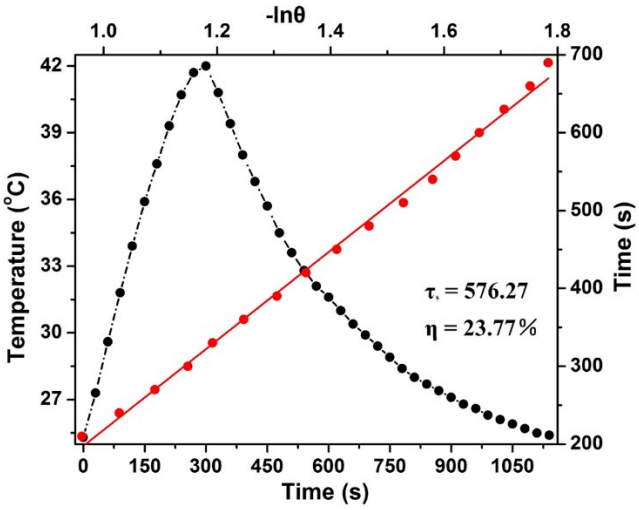

Fig. S8 Calculation of the photothermal-conversion efficiency value of CSNPs/NO under 1064 nm laser irradiation.

The photothermal conversion efficiency (η) was calculated according to the eq. 1:

$$\eta = \frac{hS(T_{max} - T_{surr}) - Q_0}{I(1 - 10^{-A})} \quad (1)$$

Where h is the heat transfer coefficient, S is the surface area of the container, T_{max} is the steady state maximum temperature, T_{surr} is the ambient temperature of the surroundings, Q_0 is the baseline energy input by the solvent, I is the laser power, and A is the absorbance of CSNPs/NO solution at 1064 nm. The value of hS is calculated by eq. 2:

$$hS = \frac{m_d C_d}{\tau_s} \quad (2)$$

Where τs is the characteristic thermal time constant (Fig. S7), the mass of the m_d and

C_d are the mass and heat capacity of water, respectively. The heat energy(Q_0) of the sample container and solvent without CSNPs/NO were measured independently using the eq. 3:

$$Q_0 = hS(T_{max} - T_{surr}) \quad (3)$$

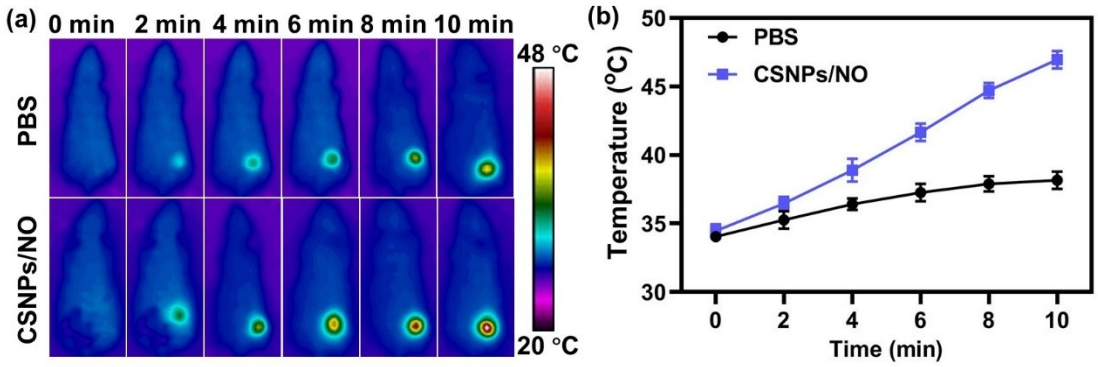

Fig. S9 IR thermal images (a) and the corresponding temperature change curves (b) of tumor-bearing mice after intravenous injection by PBS or CSNPs/NO under 1064 nm laser irradiation with a power density of 1 W cm^{-2}.

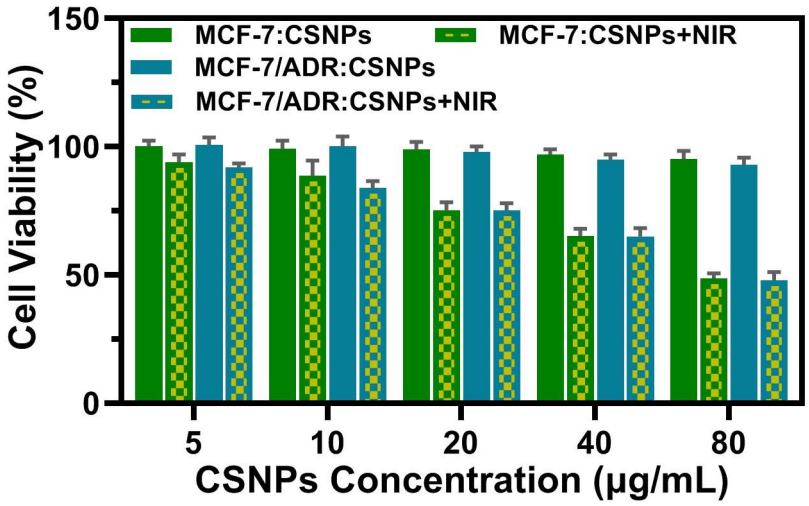

Fig. S10 Cytotoxicity of CSNPs incubated with MCF-7 and MCF-7/ADR cells and adding with or without 1064 nm laser irradiation.

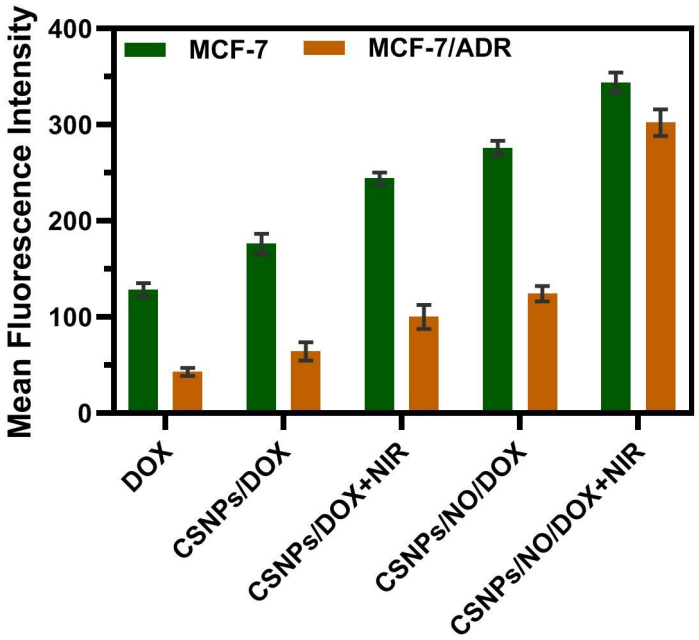

Fig. S11 Flow cytometry quantitative analysis of cellular uptake of DOX in MCF-7 cells and MCF-7/ADR cells after treated with free DOX, CSNPs/DOX, CSNPs/DOX+NIR, CSNPs/NO/DOX, and CSNPs/NO/DOX+NIR for 4h incubation (1064 nm laser, 1.0 W cm^{-2} for 10 min).

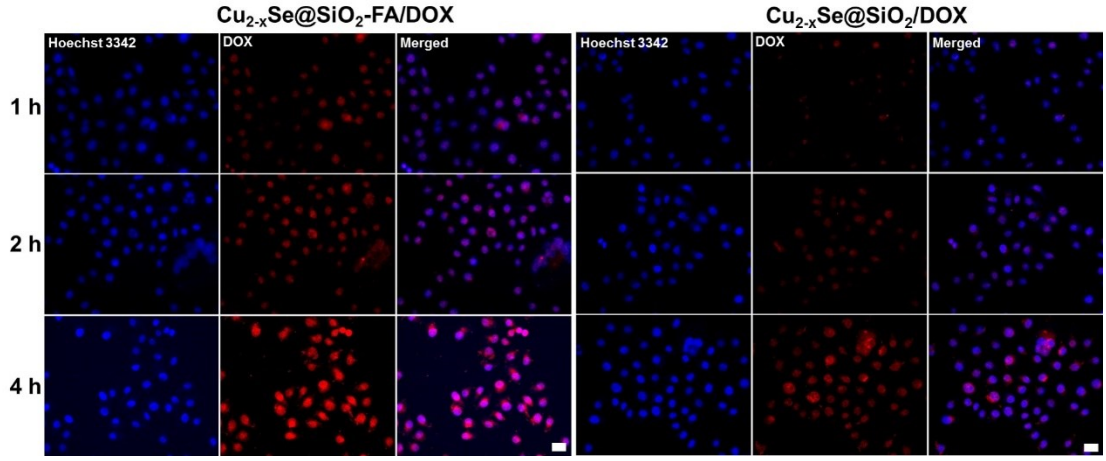

Fig. S12 CLSM images of $Cu_{2-x}Se@SiO_2$-FA/DOX (CSNPs/DOX) and $Cu_{2-x}Se@SiO_2$/DOX (CSNPs/DOX-FA) uptake by MCF-7/ADR cells for 1 h, 2 h and 4 h. Scale bar = 20 μm

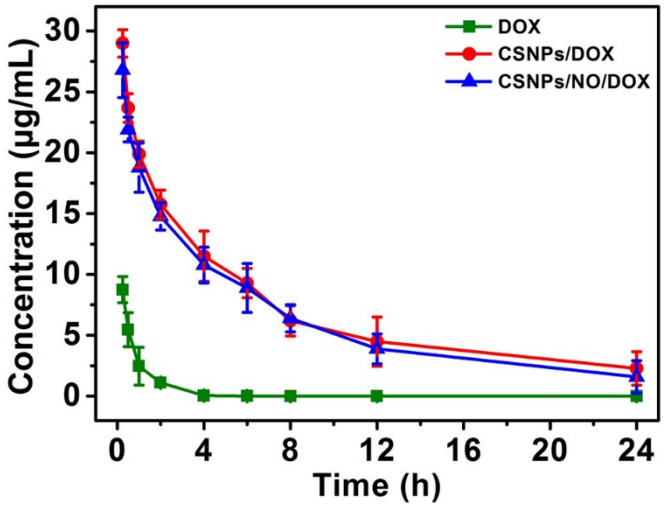

Fig. S13 Representative plasma concentration-time profiles of free DOX, CSNPs/DOX and CSNPs/NO/DOX after i.v. injection into rats. The data are presented as the average ± standard error (n = 4).

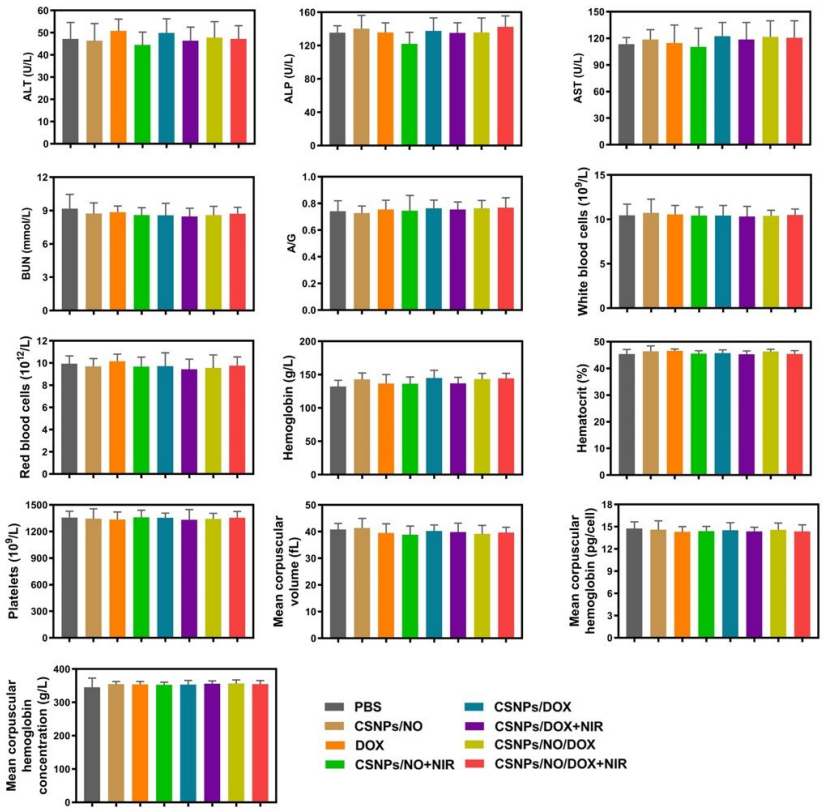

Fig. S14 Blood analysis data of mice 30 days after the different treatments. These findings did not indicate a trend of toxicity. ALT = alanine aminotransferase; AST = aspartate aminotransferase; ALP = alkaline phosphatase; TP = total bilirubin; BUN = blood urea nitrogen.

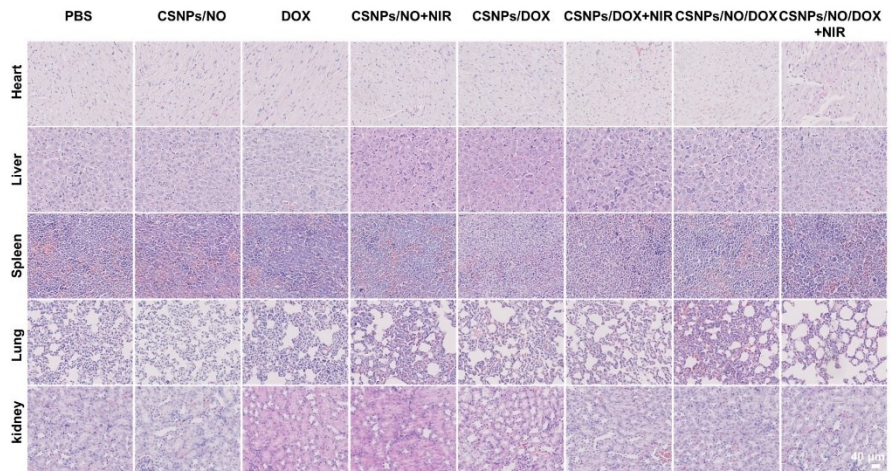

Fig. S15 H&E staining assay of normal organs obtained at the end of tumor therapeutic experiments. The organs were harvested from MCF-7/ADR tumor-bearing nude mice at the 30 day. Examined organs included lung, heart, kidney, spleen, and liver. No obvious organ damage was observed for the different groups.

Table S1. Pore size, pore volume and BET surface of CSNPs and CSNPs/NO.

Sample	Pore size (nm)	Pore volume (cm^3/g)	BET surface area (m^2/g)
CSNPs	2.77	0.85	273
CSNPS/NO	2.57	0.81	256

Table S2. Hydrodynamic size of CSNPs/NO measured in PBS (pH 7.4), cell culture media DMEM without FBS and DMEM supplemented with 10% FBS.

CSNPs/NO	PBS	DMEM	DMEM 10% FBS
Hydrodynamic size [nm] (PDI)	133 (0.17)	141 (0.18)	152 (0.15)